Formation of low-δ18O magmas of the Kangerlussuaq Intrusion by addition of water derived from dehydration of foundered basaltic roof rocks

6 AUTHORS, INCLUDING:

Morten S. Riishuus
University of Iceland
61 PUBLICATIONS 110 CITATIONS

Chris Harris
University of Cape Town
156 PUBLICATIONS 2,318 CITATIONS

Christian Tegner
Aarhus University
113 PUBLICATIONS 1,431 CITATIONS

J. Richard Wilson
Aarhus University
56 PUBLICATIONS 780 CITATIONS

CrossMark

ORIGINAL PAPER

Formation of low-δ^{18}O magmas of the Kangerlussuaq Intrusion by addition of water derived from dehydration of foundered basaltic roof rocks

Morten S. Riishuus[1] · **Chris Harris**[2] · **David W. Peate**[3] · **Christian Tegner**[4] · **J. Richard Wilson**[4] · **C. Kent Brooks**[5]

Abstract The Kangerlussuaq Intrusion in East Greenland is concentrically zoned from quartz nordmarkite (quartz syenite) at the margin, through pulaskite, to foyaite (nepheline syenite) in the centre, with no apparent intrusive contacts. The δ^{18}O values of coexisting minerals are consistent with oxygen isotope equilibrium at magmatic temperatures. Most of the intrusion formed from low-δ^{18}O magma; magma δ^{18}O values generally increased upwards from about 3.3 ‰ in the quartz nordmarkites to 5.6 ‰ in the foyaites. The lowest magma δ^{18}O value of about −1.0 ‰ is from the upper part of the nordmarkites, where there is a high concentration of foundered basaltic xenoliths (stoped from the roof of the intrusion). The amphiboles in the syenites have δD values that range from those typical of hydrous mantle-derived minerals to much lower values (−86 to −157 ‰), as do whole-rock samples of xenolith and country rock (−125 to −148 ‰). The low magma δ^{18}O and δD values are consistent with continuous incorporation, exchange and upward escape of low-δ^{18}O and δD fluids released from stoped basaltic roof material. Mass balance suggests that the integrated amount of water involved was 7 wt% of the volume of the magma, but locally reached 30 wt% water. The requirement for large amounts of water with low δ^{18}O value is satisfied only if the foundered basalt contained most of its water in cavities as opposed to hydrous minerals. Even with this requirement, the volume of stoped basalt would have been equal to the volume of the magma. Repeated recharge of the residual magma with progressively less contaminated silica undersaturated melt resulted in a gradual shift across the low-pressure thermal divide. Crystallisation was suppressed by the depression of the liquidus due to water saturation of the residual magma (pH$_2$O ~1 kbar).

Keywords Low-δ^{18}O magma · Syenite petrogenesis · Petrogeny's residua system · East Greenland

Introduction

Low-δ^{18}O magmas have δ^{18}O values that are less than the 5.7 ‰ expected for a mantle-derived magma (e.g. Bindeman 2008). Such magmas are generally found in areas where ambient surface precipitation has extreme negative δ^{18}O values and represent assimilation and/or melting of altered volcanic material (e.g. Taylor 1986). Low-δ^{18}O magmas are, in nearly all cases, felsic because of the requirement that crust is recycled. Iceland provides the exception, where both low-δ^{18}O basalts and rhyolites occur. The East Greenland volcanic rifted margin (Fig. 1a) is part of the Palaeogene North Atlantic Igneous Province. Low-δ^{18}O rocks, which exchanged with circulating meteoric water at high temperature, are common along its margins (e.g. Taylor and Forester 1979; Brandriss et al. 1996).

✉ Morten S. Riishuus
riishuus@hi.is

1 Nordic Volcanological Center, Institute of Earth Sciences, University of Iceland, Sturlugata 7, 101 Reykjavík, Iceland

2 Department of Geological Sciences, University of Cape Town, Rondebosch 7700, South Africa

3 Department of Earth and Environmental Sciences, University of Iowa, 121 Trowbridge Hall, Iowa City, IA 52242, USA

4 Department of Geoscience, Aarhus University, Høegh-Guldbergs Gade 2, 8000 Århus C, Denmark

5 Natural History Museum of Denmark, University of Copenhagen, Øster Voldgade 5-7, 1350 Copenhagen K, Denmark

Springer
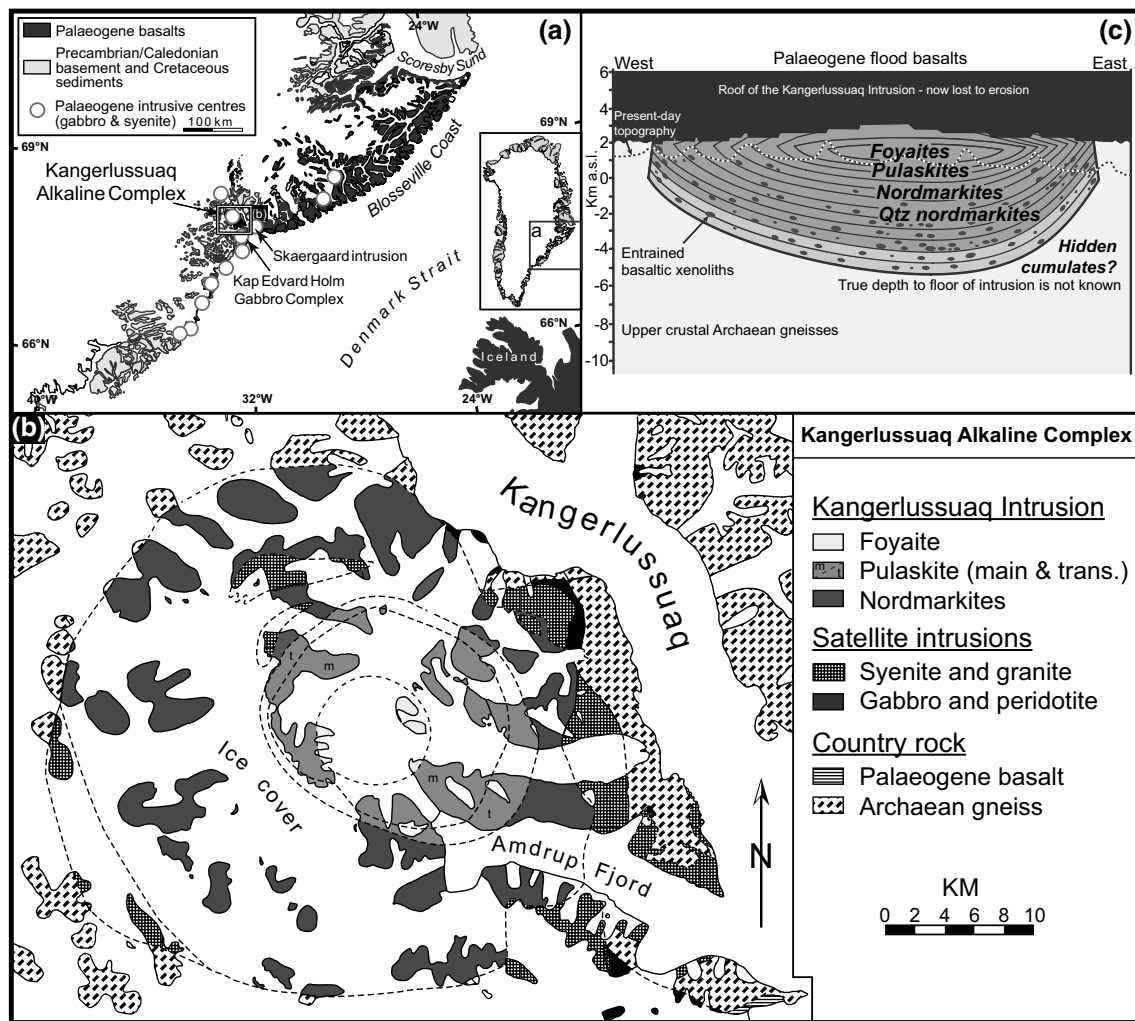
Fig. 1 a Map of central east Greenland showing the distribution of Palaeogene flood basalts, intrusive centres (gabbros and syenites) and older basement rocks. **b** Map of the Kangerlussuaq Alkaline Complex west of the Kangerlussuaq Fjord (after Kempe et al. 1970). **c** Idealised section across the Kangerlussuaq Intrusion, modified from Riishuus et al. (2006)

One example is the Sandwich Horizon of the Skaergaard Intrusion that, following crystallisation, underwent hydrothermal exchange and was subsequent remelted to produce a low-δ^{18}O magma (Wotzlaw et al. 2012). However, large intrusions in the North Atlantic Igneous province that crystallised from low-δ^{18}O magma have not yet been described.

Many of the Palaeogene extrusive and intrusive rocks from East Greenland have acquired low δ^{18}O and δD values by interaction with hydrothermal fluids of meteoric origin after crystallisation (Sheppard et al. 1977; Taylor and Forester 1979; Rose 1989; Nevle et al. 1994; Brandriss et al. 1995, 1996). Worldwide, low-δ^{18}O magmas are less common than low-δ^{18}O rocks, because they appear to involve melting or assimilation of low-δ^{18}O rocks that are themselves unusual (e.g. Taylor 1986; Bindeman 2008).

Direct addition of water to magma has generally been discounted as a mechanism of generating low-δ^{18}O magmas because the rate of diffusion of water into magma is thought to be too slow (e.g. Taylor 1986). However, Taylor (1986) suggested that incorporation of hydrous basaltic xenoliths could be an efficient way of adding water to magma, because volatiles liberated from the dehydrating xenoliths would be absorbed by the magma. Evidence for dehydration and partial melting of altered basaltic xenoliths has been recognised in gabbroic plutons in East Greenland such as the Skaergaard Intrusion and Kap Edvard Holm Complex (Taylor and Forester 1979; Brandriss et al. 1996). Similar xenoliths are found in the syenitic Kangerlussuaq Intrusion (Wager 1965; Kempe et al. 1970; Riishuus et al. 2008). This intrusion (~51 Ma, Tegner et al. 2008) in East

Greenland is famous for showing a gradual transition from quartz syenite (marginal) to upper nepheline syenite (central) (Wager 1965), and the magmatic evolution therefore appears to cross the thermal barrier in petrogeny's residua system (Schairer 1950; Tuttle and Bowen 1958).

In this study, the oxygen and hydrogen isotope compositions of coexisting primary minerals from the Kangerlussuaq Intrusion are used to show that the majority of the intrusion crystallised from low-δ^{18}O magma. A combination of whole-rock data from the country rock gneisses, and basaltic xenoliths, are used to examine the origin and amount of water that could have resulted in the formation of these low-δ^{18}O magmatic rocks. Finally, the role of fluids in the transition from silica oversaturated to undersaturated magma during the evolution of the magma chamber is evaluated.

Geological background

The Palaeogene magmatism of the North Atlantic Igneous Province is considered to be a consequence of the initial activity of the Iceland mantle plume and the onset of rifting of the North Atlantic (e.g. Brooks 1973; Saunders et al. 1997). Magmatism along the East Greenland volcanic rifted margin (Fig. 1a) (e.g. Brooks and Nielsen 1982a; Nielsen 1987; Larsen et al. 1989; Pedersen et al. 1997) includes (1) the ~62–58 Ma Lower Basalts, Nansen Fjord and Urbjerget formations that are related to the thermal impact from the initial arrival of the mantle plume (e.g. Hansen et al. 2002; Storey et al. 2007); (2) the 56–55 Ma Plateau Basalts that are related to decompression melting during continental rifting (e.g. Storey et al. 2007); and (3) post-break-up ~53–47 Ma gabbroic and syenitic intrusions, and alkaline lavas, that may be related to passage of the continental margin over the plume axis (e.g. Peate et al. 2003; Riishuus et al. 2005; Tegner et al. 2008).

The country rocks of the Kangerlussuaq area (Brooks and Nielsen 1982b) are dominated by Archaean basement gneiss, but also include rocks of Caledonian age and Late Cretaceous to early Palaeogene sedimentary rocks (Fig. 1a). These rocks are overlain by the Palaeogene volcanic pile. In the Kangerlussuaq area, this stratigraphic sequence was intruded by a number of Palaeogene intrusive rocks including the gabbroic Kap Edvard Holm Complex, the Skaergaard Intrusion, and the felsic Kangerlussuaq Intrusion and its related satellite intrusions (Riishuus et al. 2006) (Fig. 1a, b).

Geology of the Kangerlussuaq Intrusion

Field relations

The Kangerlussuaq Intrusion was emplaced in the form of a 30- to 35-km-diameter asymmetric lopolith at the unconformity between Archaean gneiss and Palaeogene flood basalts (e.g. Wager 1965; Riishuus et al. 2008) (Fig. 1b, c). It covers an area of ~800 km^2 and therefore constitutes the majority of the exposed part of the Kangerlussuaq Alkaline Complex (e.g. Deer and Kempe 1976; Riishuus et al. 2006) (Fig. 1b). The intrusion shows a gradation (Fig. 1b) from *foyaites* (>5 % feldspathoids) in the centre, through the *main pulaskites* (<5 % feldspathoids), *transitional pulaskites* (quartz and feldspathoids both absent), *nordmarkites* (<10 % quartz) to *quartz nordmarkites* (~10 % quartz) at the margin (Wager 1965). A notable feature of the quartz nordmarkites is the sporadic presence of trains of huge, elongated, basaltic xenoliths interpreted as being derived from the lava flows that make up the chamber roof (Wager 1965; Kempe et al. 1970; Riishuus et al. 2008). The basaltic xenoliths dip at 30°–60° towards the centre of the intrusion and are presumed to outline the geometry of the chamber floor (Fig. 1c). These xenoliths vary in size from small fragments to hundreds of metres across and, in places, are often present in zones where xenoliths are more abundant than the host magmatic rock (Wager 1965). A few basaltic xenoliths occur in the outer part of the main pulaskites, but they are absent from the inner, silica undersaturated part of the intrusion. The geochemical composition of the basaltic xenoliths is consistent with them belonging to the Palaeogene Lower Basalts (Riishuus et al. 2008). The locally developed modal layering in the quartz nordmarkites and igneous lamination in the nordmarkites and pulaskites dip 30°–60° towards the centre of the intrusion, consistent with a cumulate origin. The intrusion can, therefore, be considered as a layered intrusion in which crystal settling took place on the chamber floor (Wager 1965). The absence of basaltic xenoliths from the inner part of the Kangerlussuaq Intrusion led Riishuus et al. (2008) to suggest that at this stage the magma became isolated from the overlying basalt pile as a result of downward crystallisation from the roof of the chamber which was, at this stage, greatly reduced in size.

Petrogenesis

Wager (1965), Kempe and Deer (1976) and Pankhurst et al. (1976) argued that the Kangerlussuaq Intrusion crystallised initially from a magma of quartz trachyte composition, but they were not able to explain fully the gradual transition from silica over- to undersaturation. Wager (1965) suggested an origin for the quartz trachyte magma by partial melting and alkali metasomatism of the basement, whereas Kempe and Deer (1976) favoured differentiation from alkali olivine basalt. In contrast to these earlier models, Brooks and Gill (1982) suggested that the foyaites formed by fractional crystallisation of alkali basalt or nephelinite

magmas, with the pulaskites and nordmarkites reflecting the increasing effect of contamination by the country rock.

On the basis of Sr, Nd, Hf and Pb isotope data and amphibole compositions, Riishuus et al. (2008) suggested that the effects of crustal contamination diminished from the evolved quartz nordmarkites (~20:80 crust–mantle mixing ratio) to the more primitive foyaites (~10:90 crust–mantle mixing ratio), in agreement with Brooks and Gill (1982). The lack of xenoliths of gneiss in the nordmarkites suggests that most of crustal contamination took place either prior to intrusion of the magma, or below the level of present exposure. Riishuus et al. (2008) favoured a model where the nordmarkitic magma formed as a result of assimilation of the roof zone by a large, stratified, mildly undersaturated alkaline basaltic magma chamber underlying the Kangerlussuaq Intrusion. There is a large positive magnetic anomaly over the Kangerlussuaq Alkaline Complex (Verhoef et al. 1996) that is consistent with this interpretation. Emplacement of the nordmarkitic magma into the uppermost crust led to formation of the Kangerlussuaq Intrusion magma chamber that stoped into the overlying basalt pile. Repeated recharge of the chamber by melt from increasingly deeper parts of the underlying chamber, combined with progressive armouring of the conduit and chamber walls, resulted in the formation of successively less crustally contaminated cumulates.

In the model proposed by Riishuus et al. (2008), nordmarkitic magma formed during assimilation of basement gneiss in the roof zone of a large, 'staging' magma chamber at depth, which was stratified from mildly undersaturated alkaline basalt to phonolite. The nordmarkitic magma was tapped from this chamber and emplaced in the uppermost crust to initiate formation of the Kangerlussuaq Intrusion.

Sample details and analytical methods

The stratigraphic position of samples (Fig. 2) has been inferred from their locations relative to a section through the centre of the intrusion based on the asymmetric, saucer-shaped structure (Fig. 1b, c; Riishuus et al. 2008). Quartz, alkali feldspar and pyroxene/amphibole were separated from the Kangerlussuaq Intrusion rocks by a combination of magnetic separation, heavy liquid separation and hand picking, with an estimated purity of >95 %. Because pyroxene and amphibole are intimately associated, separation of these two minerals was not possible, and mixtures were analysed. This does not influence the interpretation, because the expected fractionation between amphibole and pyroxene at magmatic temperatures is small (Zheng 1993a, b). Whole-rock samples of country rocks (basement gneisses and mafic dykes) and basaltic xenoliths were also analysed. Full petrographic details and compositional data on all
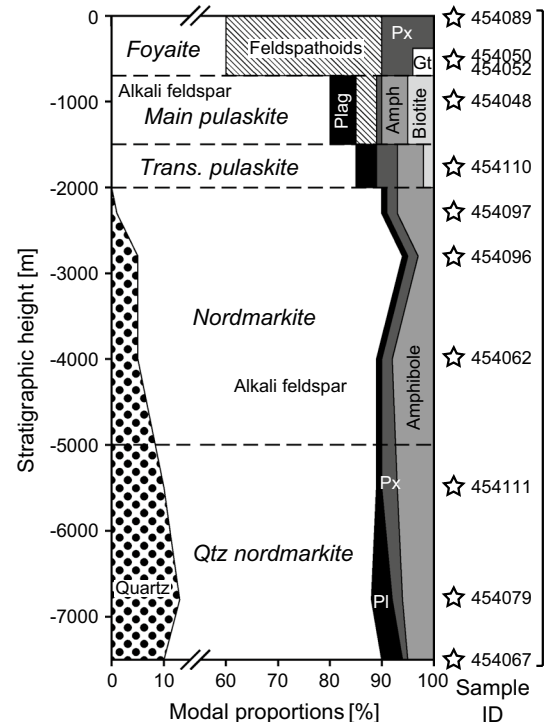
Fig. 2 Modal proportions of the main mineral phases that define the lithological variation of the Kangerlussuaq Intrusion (Riishuus et al. 2008) against stratigraphic height. The *star symbols* indicate the approximate stratigraphic position of samples used in the present study. See Riishuus et al. (2008) for more details on sample descriptions and locations

samples can be found in Riishuus et al. (2008). Oxygen and hydrogen isotope analyses were carried out at the University of Cape Town using a Finnigan MAT252 mass spectrometer in dual-inlet mode. Oxygen was produced from ~10 mg of powdered sample using the 'conventional' closed Ni tube extraction technique (Vennemann and Smith 1990) using ClF_3 as reagent. The data are reported in δ notation, where $\delta^{18}O = 1000 \times (^{18}O/^{16}O_{sample}/^{18}O/^{16}O_{standard} - 1)$. The NBS-28 quartz standard was run twice with each sample batch and used for correction to the V-SMOW (standard mean ocean water) scale using a value of 9.64 ‰ for NBS-28. The average difference between 12 duplicate pairs of NBS-28 was 0.27 ‰, which approximates to a 1σ precision of ±0.15 ‰.

Hydrogen was extracted from 100 mg of amphibole/pyroxene, 200 mg of whole-rock gneiss or 25 mg of whole-rock basalt using the method of Vennemann and O'Neil (1993). The water extracted from each sample was converted to H_2 using 100 mg of low-blank 'Indiana' Zn. Samples were degassed on the vacuum line at 200 °C prior to pyrolysis. An internal water standard (CTMP1, δD = −9 ‰) was used to calibrate the data to the SMOW scale and a second water standard DML (δD = −300 ‰)

was used to correct for scale compression (Coplen 1988). The internal standard CG biotite gave an average value of -58.3 ± 2.6 ‰ (1σ, $n = 6$) during the period of analysis. Water contents were determined either from the voltage measured on the mass 2 collector or (in the case of large samples) from the pressure measured during sample inlet using identical inlet volume to standards of known number of micromoles. Repeated measurements of water standards of known mass suggest that the typical relative error for the water content is 3 %. The water content of CG biotite measured during the course of this work was 3.78 % $\pm$ 0.06 (1σ, $n = 6$). The accepted δD value for CG biotite is -59 ‰ with a water content of 3.70 wt%. During the initial analytical work, it was observed that many of the amphibole/pyroxene mixtures gave extremely negative δD values, some as low as -269 ‰. Similarly, low δD values were not observed for the bulk-rock basalt or gneiss samples. One possibility is that the high fluorine content of the amphibole affected the Zn reduction, and experiments were done with variable sample/Zn ratios. No water remained after the Zn reduction, and the low δD values were not, therefore, the result of fractionation between H_2 and residual water. Approximately 100 mg aliquots of amphibole 454097 were processed in the normal way and the water extracted reduced with 100, 200, 300 and 400 mg of Zn. The δD values obtained were -338, -255, -145 and -179 ‰, respectively. Water from CG biotite reacted with 100, 200, 300 and 400 mg Zn gave δD values of -63, -58, -56 and -59 ‰, respectively. Varying the proportion of Zn to sample water does not, therefore, affect the δD value of the comparatively fluorine-free CG biotite, but high

Zn/water ratios appear necessary to obtain reliable data for the fluorine-rich amphiboles. It is not known why the 300 and 400 mg Zn analyses of the amphibole 454097 differ by 34 ‰. The δD value obtained with 300 mg Zn of -145 ‰ is very similar to the values obtained for the whole-rocks, which suggest that it is correct. All amphibole δD values were, therefore, obtained from about 100 mg sample using 300 mg of Zn. In the case of 4 samples, sufficient material existed for a duplicate analyses and the difference in δD value between duplicates averaged 10 ‰. The δD values determined on the F-rich amphiboles are therefore less precise than the 'normal' standard, but this does not influence the interpretation.

Oxygen and hydrogen isotope data

The Archaean basement samples have whole-rock $\delta^{18}O$ values of 7.0–8.1 ‰ (Table 1), which are fairly typical of Archaean basement worldwide (e.g. Vennemann and Smith 1992; Fagereng et al. 2008). The two mafic dyke samples have $\delta^{18}O$ values of 3.2 and 5.4 ‰, and the three basalt xenoliths have highly variable whole-rock $\delta^{18}O$ values of -3.2, $+3.8$ and $+4.6$ ‰. It should be noted that all of the non-basement mafic rocks have $\delta^{18}O$ values that are lower than expected for mantle-derived magmas (5.7 ± 0.5 ‰, Eiler 2001).

The minerals of the Kangerlussuaq Intrusion have variable $\delta^{18}O$ values, from those that are appropriate for a mantle-derived magma to lower values that are in some cases negative. The $\delta^{18}O$ values of the groundmass alkali feldspar

Table 1 Oxygen isotope compositions of minerals, whole-rocks and magmas from the Kangerlussuaq Intrusion

Sample	Rock type	Strat. (m)	$\delta_{Afs, phx}$	$\delta_{Afs, gm}$	δ_{Qtz}	$\delta_{Am/Px}$	δ_{magma}				Sample	Rock type	δ_{wr}
							Afs, phx	Afs, gm	Qtz	Am/Px			
454089	F	0		6.0		3.4^p		5.6		5.6	454041	BG	8.1
454050	F	-500		4.3		3.3^p				5.5	454042	BG	7.3
454052	F	-500		5.3		2.3^p		4.9		4.5	454043	BG	7.9
454048	MP	-1000		5.0		2.1		4.6		4.6	454073	BG	7.6
454110	TP	-1750		4.2		1.3		3.8		3.9	454074	MB	7.0
454097	N	-2300	3.0	3.1		0.8	2.6	2.8		3.4	454075	BG	8.1
454096	N	-2800	-0.4	-0.5	0.7	-2.4	-0.8	-0.9	-1.2	0.2	454080	BX	3.8
454062	N	-4000	4.6	4.2	5.8	2.0	4.2	3.9	4.0	4.6	454081	BX	-3.2
454111	QN	-5500	3.9	4.1	5.2	2.2	3.5	3.7	3.3	4.8	454091	MD	3.2
454079	QN	-6800	3.4	2.7	4.7	2.1	3.0		2.9	4.7	454094	BX	4.6
454067	QN	-7500	4.3	3.7	4.6	1.2	3.9	3.4	2.8	3.8	454098	MD	5.4

Mixed amphibole/pyroxene analyses marked p are pure pyroxene analyses. The following values of $\Delta_{mineral-melt}$ have been applied: $\Delta_{quartz-magma} = 1.84$ ‰, $\Delta_{alkali\ feldspar-magma} = 0.37$ ‰, $\Delta_{pyroxene-magma} = -2.21$ ‰ and $\Delta_{amphibole/pyroxene-magma} = -2.59$ ‰. See text for discussion of $\Delta_{mineral-melt}$ values

F foyaite, MP main pulaskite, TP transitional pulaskite, N nordmarkite, QN quartz nordmarkite, BX basaltic xenolith, MD mafic dyke, BG local basement gneiss, MB basement metabasite, $Strat$ stratigraphic height, phx phenocryst, gm groundmass

range from −0.5 to +6.0 ‰, and where available, alkali feldspar phenocrysts have very similar δ¹⁸O values to the groundmass feldspar (Table 1). The pyroxene/amphibole mixtures have a similar range of slightly lower δ¹⁸O values (−2.4 to +3.4 ‰), and quartz extracted from about half the analysed samples has a range in δ¹⁸O value from +0.7 to +5.8 ‰.

Mineral separates were analysed in preference to whole-rocks because the latter are more susceptible to secondary alteration (e.g. Taylor 1968). Petrographic observations indicate that the alkali feldspar, which is present throughout the intrusion, is only slightly affected by secondary alteration. Nevertheless, because alkali feldspar is known to be susceptible to alteration, we have analysed coexisting quartz (when present) and pyroxene/amphibole to assess the degree of O-isotope equilibrium within samples. Quartz does not undergo low-temperature (<300 °C) exchange of oxygen with a fluid in the absence of deformation and is resistant to alteration at low temperatures (e.g. Taylor 1968).

Magmatic equilibrium is characterised by an array on a δ–δ diagram (Fig. 3) with a constant per mil difference (Δ) between the two minerals that, because Δ depends on temperature, represents a constant temperature. For magmatic temperatures, values of Δ are relatively small, e.g. 0.7 (quartz-alkali feldspar) and 2.2 (quartz-hornblende) at 900 °C. Minor deviations from the equilibrium array may be due to the effects of 'closure' to O diffusion at different temperatures for different minerals (e.g. Gregory and Criss 1986). A series of rocks that have been affected by substantial sub-solidus exchange with external fluids will generally form a disequilibrium array that crosses the equilibrium line. This is because of the greater susceptibility of one of the minerals to equilibrate with the fluid.

From the quartz nordmarkites through the pulaskites, the amphibole/pyroxene mixtures are dominated by sodic–calcic amphiboles with full or near-full A sites ((magnesio)katophorite, (ferro)richterite, (magnesio)arfvedsonite; Riishuus et al. 2008). Zheng (1993b) offers a number of quartz–amphibole isotopic equilibrium fractionation
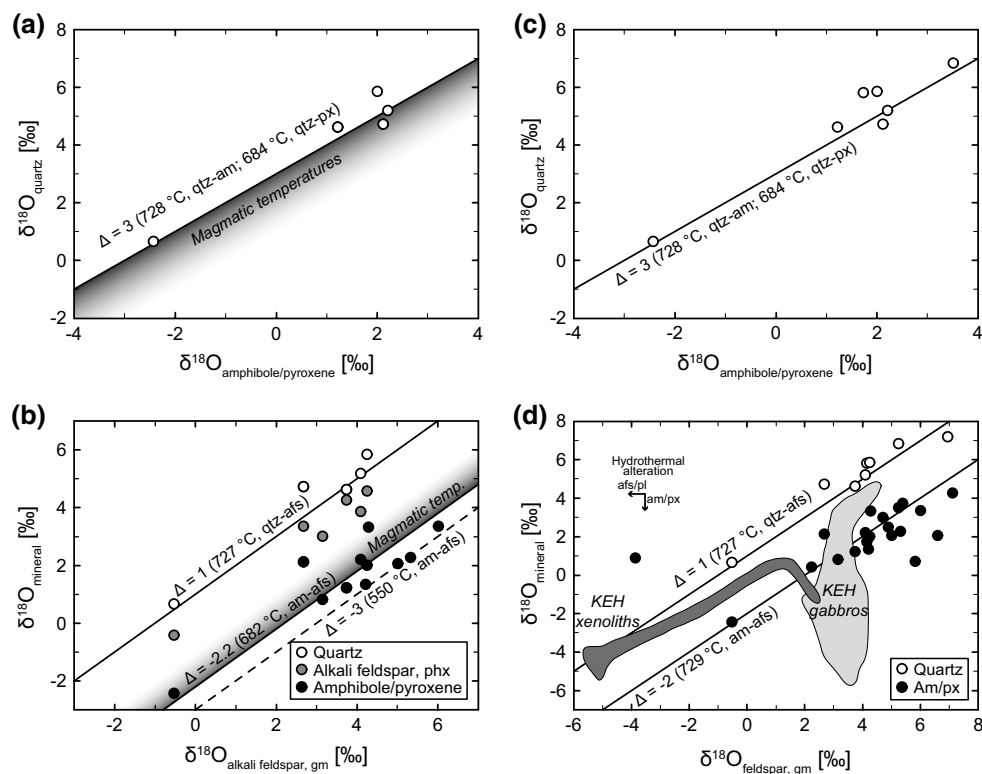
Fig. 3 Mineral–mineral δ–δ plots for coexisting mineral pairs: **a** quartz δ¹⁸O versus amphibole/pyroxene δ¹⁸O and **b** quartz, alkali feldspar phenocryst and amphibole/pyroxene δ¹⁸O versus groundmass alkali feldspar δ¹⁸O for the Kangerlussuaq Intrusion. **c** Quartz δ¹⁸O versus amphibole/pyroxene δ¹⁸O value and **d** quartz, feldspar phenocryst and amphibole/pyroxene δ¹⁸O versus groundmass feldspar δ¹⁸O values for rock samples of the Kangerlussuaq Alkaline Complex (Riishuus et al. 2006; this study). The fields of Kap Edvard Holm Complex (KEH) metabasaltic xenoliths and gabbros in **d** are from Brandriss et al. (1996). Oxygen isotope equilibrium lines are shown with temperatures calculated using the equations of Clayton et al. (1989) for quartz–feldspar, Chiba et al. (1989) for quartz–diopside and Lackey et al. (2008) for quartz–amphibole (hornblende). The amphibole–alkali feldspar equilibrium line is constructed by combining fractionation equations for quartz–alkali feldspar and quartz–amphibole

Table 2 Hydrogen isotope compositions of amphiboles and whole-rocks from the Kangerlussuaq Intrusion

Sample	Rock type	Strat. (m)	Material	δD	H_2O^+ (wt%)	Am–Px (prop. %)	Am H_2O^+ (wt%)
454048	MP	−1000	Am/Px	−113	0.96	83–17	1.16
454110	TP	−1750	Am/Px	−86 (8)	0.15 (.00)	14–86	1.10
454096	N	−2800	Am/Px	−147 (8)	0.61 (.01)	60–40	1.01
454062	N	−4000	Am/Px	−157	0.63	80–20	0.79
454111	QN	−5500	Am/Px	−157 (2)	0.56 (.01)	70–30	0.80
454079	QN	−6800	Am/Px	−157	0.47	50–50	0.93
454067	QN	−7500	Am/Px	−143 (3)	0.84 (.00)	83–17	1.01
454074	MB		wr	−133	0.51		
454075	BG		wr	−148	0.45		
454094	BX		wr	−124	1.82		

Values in parentheses deviate from mean where duplicate analyses were performed. The material analysed was either amphibole + pyroxene (Am/Px) or whole-rock (wr). The water content of the amphibole has been estimated from the water content of the mixture and the proportion of amphibole present in the mixture

F foyaite, *MP* main pulaskite, *TP* transitional pulaskite, *N* nordmarkite, *QN* quartz nordmarkite, *BX* basaltic xenolith, *MD* mafic dyke, *BG* local basement gneiss, *MB* basement metabasite, *Strat* stratigraphic height

factors, including hornblende (calcic amphibole with optional A site), pargasite (calcic amphibole with Na in A site) and riebeckite (alkali amphibole with empty A site). With none of the available quartz–amphibole pairs directly suitable for the amphibole compositional range of the Kangerlussuaq Intrusion, we prefer to use the quartz–amphibole (hornblende) isotopic equilibrium fractionation factor of Lackey et al. (2008). For the Kangerlussuaq Intrusion, a plot of quartz $\delta^{18}O$ versus amphibole/pyroxene $\delta^{18}O$ compositions for coexisting pairs shows positive correlation and an average $\Delta_{quartz–amp/px}$ of 3 (Fig. 3a); this corresponds to a temperature of 728 °C for quartz–amphibole (hornblende) (Lackey et al. 2008) and 684 °C for quartz–pyroxene (diopside) (Chiba et al. 1989). For comparison, a per mil difference Δ of ~3 corresponds to temperatures of 690 and 755 °C for quartz–hornblende and quartz–pargasite pairs, respectively (Zheng 1993b). Similar plots for quartz, amphibole/pyroxene and feldspar phenocryst versus groundmass feldspar show arrays that are consistent with equilibrium at high temperatures (Fig. 3b). Two samples (454050 and 454079) have feldspar–amphibole/pyroxene pairs that plot ~1.2 ‰ above the $\Delta = −2.2$ ‰ amphibole–alkali feldspar fractionation line at 682 °C. This is consistent with these feldspars having experienced moderate alteration with lowering of $\delta^{18}O$ by 1–1.5 ‰. Data for the Kangerlussuaq Alkaline Complex as a whole (Riishuus et al. 2006) are shown in Fig. 3c, d. Although there is a somewhat larger range of data, the δ–δ plot for quartz versus amphibole/pyroxene (the two minerals that are most resistant to alteration) is clearly consistent with O-isotope equilibrium at magmatic temperatures (Fig. 3c). In contrast to the Kap Edvard Holm Complex (steeply dipping, disequilibrium fractionation array in Fig. 3d) (Brandriss et al.

1996) and the Skaergaard Intrusion (Taylor and Forester 1979), the Kangerlussuaq rocks (with a few exceptions) do not appear to have exchanged any significant oxygen with external hydrothermal fluids during slow cooling.

It can be assumed that the pyroxene component of the amphibole/pyroxene mixture separated from the intrusive rocks does not contribute to the δD values, which range from −157 to −86 ‰ (Table 2). The whole-rock δD value of one basaltic xenolith is −124 ‰, whereas two Archaean basement samples gave δD values of −133 and −148 ‰. The water contents measured during the H-isotope analysis (see above) are relatively low for the country rocks (0.51 and 0.45 wt%), and the basalt xenolith has 1.82 wt% water. The water content of the amphibole/pyroxene mixtures combined with visual estimates of the proportion of amphibole to pyroxene gives amphibole water contents that range from 0.79 to 1.16 wt%. None of the amphiboles has water content that approaches the theoretical maximum of about 2 wt%, which suggests the presence of significant amounts of F and/or Cl.

The $\delta^{18}O$ and δD values, and amphibole water contents, for the intrusion (Tables 1, 2) are plotted against inferred stratigraphic height in Fig. 4. The $\delta^{18}O$ values of the separated minerals are either approximately constant (amphibole/pyroxene) or increase slightly (alkali feldspar and quartz) from the stratigraphically lowest quartz nordmarkites (−7500 to −6800 m) to −4000 m in the nordmarkites (Fig. 4a). At −2800 m within the nordmarkites, one sample has lower mineral $\delta^{18}O$ values (quartz +0.7 ‰, the other minerals −ve). Above this level, the $\delta^{18}O$ values of both alkali feldspar and pyroxene/amphibole increase systematically from the uppermost nordmarkite, through the pulaskites to the foyaite at the top of the stratigraphic
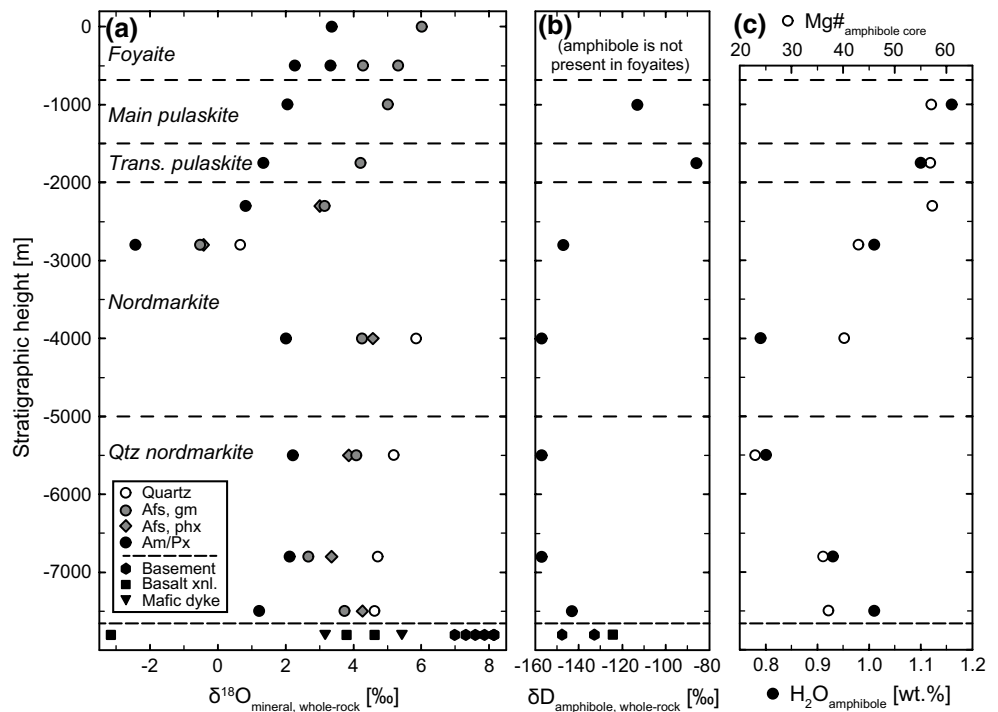
section. There are too few hydrogen isotope data to make
firm conclusions about the stratigraphic variation. The δD
values of amphibole/pyroxene in the two pulaskite samples
are less negative (−113 to −86 ‰; Fig. 4b and Table 2)
than the δD values of the nordmarkites and quartz nord-
markites (−157 to −143 ‰). The less negative δD values
above −3000 m correspond to an increase in δ^{18}O values
(Fig. 4a, b).

Discussion

Comparison to previous whole-rock O-isotope study

In an earlier study, Pankhurst et al. (1976) found that
the Kangerlussuaq foyaites had whole-rock δ^{18}O val-
ues of 3.7–4.3 ‰ (average 3.9 ‰, n = 6), whereas the
nordmarkites and quartz nordmarkites had somewhat
higher δ^{18}O values of 3.7–5.5 ‰ (average 4.5 ‰, n = 7).
Although this is the opposite to our findings of slightly
higher alkali feldspar δ^{18}O values in the foyaites than in
the nordmarkites, it is inadvisable to infer too much from
these differences. The δ^{18}O value of nepheline was not
determined, but the small fractionation between nepheline
and alkali feldspar ($\Delta_{Ne–Or}$ = 1.02 ‰ at 700 °C, Zhao and
Zheng 2003) suggests that even 30 % nepheline present
in the foyaite could not account for this difference. How-
ever, the lower whole-rock δ^{18}O values in the foyaites can
be explained by the greater susceptibility of nepheline to
alteration and lowering of its δ^{18}O value. Notwithstanding

this minor discrepancy between whole-rock and feld-
spar data, the important feature of both data sets is that
δ^{18}O values are generally lower than the 5.7 ‰ expected
for mantle-derived magmas. As is the case for our data,
feldspar, magnetite, amphibole and sphene δ^{18}O values
reported by Pankhurst et al. (1976) are consistent with
equilibrium at magmatic conditions.

In order to explain the low δ^{18}O values of the undersat-
urated rocks, Pankhurst et al. (1976) suggested that mete-
oric water with very low δ^{18}O value entered the system
directly after about 60 % crystallisation, thereby lowering
the δ^{18}O value of the magma. The precise mechanism by
which the water and magma interacted was not specified,
but the amount of water that exchanged with the magma
was estimated to be 10 wt%. Pankhurst et al. (1976) recog-
nised that not all of the water had to be present at any one
time and that the maximum amount of water dissolved in
the magma could not have exceeded 3–4 wt% in order for
P_{H2O} to remain < P_{total}. These authors further suggested that
the increase in P_{H2O} would have lowered the liquidus tem-
peratures, while maintaining a relatively high magma tem-
perature. If the magma temperature was higher than that of
the Ab–Or thermal divide, open-system processes such as
assimilation of mafic material could have driven the com-
position of the evolved residual magma towards the nephe-
line syenite minimum, although the exact mechanism was
not fully explained. The positive correlation they observed
between whole-rock δ^{18}O value and initial Sr isotope ratio
in the pulaskites and foyaites was explained by fluid-rock
exchange at low water/rock ratio in the margin of the

intrusion, which raised the $\delta^{18}O$ value and $^{87}Sr/^{86}Sr$ ratio of the groundwater before interaction with the magmatic rocks.

Although the relatively impermeable gneisses have low δD values (-148 to -133 ‰), which might be explained by minor meteoric-hydrothermal exchange, their $\delta^{18}O$ values [~7.0–8.1 ‰, this study and Pankhurst et al. (1976)] are similar to quartz feldspathic gneisses considered unaltered elsewhere in the Kangerlussuaq region (7.3–7.7 ‰, Taylor and Forester 1979). Furthermore, because there is no correlation between the $\delta^{18}O$ value of gneiss and distance from the intrusion, we argue that no hydrothermal system was established, either in the gneisses, or in the Kangerlussuaq Intrusion. As is the case in the Skaergaard Intrusion (Taylor and Forester 1979), the hydrothermal convection in the country rock was probably limited to the overlying basalts. The low $\delta^{18}O$ (-3.2 to 4.6 ‰) and δD (-124 ‰) of the basaltic xenoliths from the Kangerlussuaq Intrusion (Fig. 4a, b and Tables 1, 2) are consistent with the general view that the basalts in the region ($\delta^{18}O = -6.0$ to -4.9 ‰ and $\delta D = -163$ to -75 ‰) are hydrothermally altered (Sheppard et al. 1977; Taylor and Forester 1979; Brandriss et al. 1995, 1996).

Magma $\delta^{18}O$ and δD values

We have demonstrated that the Kangerlussuaq Intrusion minerals are generally in O-isotope equilibrium at magmatic temperatures. In order to estimate the $\delta^{18}O$ value of the magma, it is necessary to assume mineral–melt fractionation factors and to take into account changes in mineral $\delta^{18}O$ values during slow cooling (e.g. Giletti 1986; Jenkins et al. 1991). The following values of $\Delta_{mineral-magma}$ are given by Zhao and Zheng (2003): alkali feldspar 0.37 ‰, quartz 0.77 ‰ and pyroxene -1.34 ‰. Alkali feldspar constitutes ~80 % of the Kangerlussuaq rocks and should therefore not change its $\delta^{18}O$ value significantly during slow cooling. Quartz and pyroxene/amphibole will continue to exchange oxygen during cooling towards the closure temperature (~550 °C), but they will not necessarily stop diffusing at the same temperature. At 550 °C, the following fractionation factors apply $\Delta_{quartz-alkali\ feldspar} = 1.48$ ‰ (Clayton et al. 1989; Lackey et al. 2008) and $\Delta_{quartz-pyroxene} = 4.06$ (Chiba et al. 1989). The $\Delta_{quartz-amphibole}$ value of Lackey et al. (2008) is 4.44 ‰ and very similar to that of quartz–pyroxene. The difference between the measured mineral and magma $\delta^{18}O$ values is, therefore, 1.85 ‰ (quartz), -2.59 ‰ (amphibole) and -2.21 ‰ (pyroxene). For separates with mixtures of pyroxene and amphibole (all samples but the foyaites), we apply $\Delta_{quartz-amphibole}$ fractionation due to the dominance of amphibole over pyroxene (Fig. 2). Feldspars from samples 454050 and 454079 are deemed moderately altered as they have too low $\delta^{18}O$ compositions to be in equilibrium with

coexisting amphibole/pyroxene and quartz (Fig. 4a, b), and hence, calculation of magma $\delta^{18}O$ is not appropriate. Magma $\delta^{18}O$ values calculated by this approach are similar for each mineral (Table 1), and regardless of any uncertainties, there is a considerable range in the estimated magma $\delta^{18}O$ values up through the stratigraphy (-0.9 to $+5.6$ ‰, using the feldspar data).

The $\delta^{18}O$ value of the magma of 5.6 ‰ for the upper- and central-most part of the foyaite (Table 1) is consistent with a mantle origin of the magma and with radiogenic isotope data that suggest that crustal input was limited to ~10 % (Riishuus et al. 2008). Other examples of mantle-derived nepheline syenites have similar magmatic $\delta^{18}O$ values (~6 ‰, Harris and Grantham 1993; Harris 1995; Marks et al. 2004). Radiogenic isotope data from the Kangerlussuaq nordmarkites sensu lato support the hypothesis of contamination by ~20 % Archaean gneisses (Riishuus et al. 2008). The gneisses have an average $\delta^{18}O$ value of 7.81 ‰, and mantle-derived magma contaminated by 20 % of this material would have had a $\delta^{18}O$ value of 6.12 ‰. In fact, $\delta^{18}O$ values of the nordmarkites are lower (quartz $\delta^{18}O < 5.8$ ‰; magma $\delta^{18}O < 4.0$ ‰). Variations in the O-isotope composition appear, therefore, to have been decoupled from the variation in radiogenic isotopes.

If it is assumed that quartz is the mineral that is least susceptible to post-magmatic changes in $\delta^{18}O$ value, the $\delta^{18}O$ value of the magma increases gradually upwards from 2.8 ‰ at -7500 m to 4.0 ‰ at -4000 m (Fig. 5). Moving up the stratigraphy, the next sample (454096 at -2800 m) has a much lower magma $\delta^{18}O$ values of -1.2 ‰. This low $\delta^{18}O$ value was not caused by secondary alteration because the minerals in this sample are in O-isotope equilibrium. It is not known how volumetrically significant this zone of extreme ^{18}O-depletion might be; it is possible that it represents a narrow zone close to an unexposed basaltic xenolith. Above the low-$\delta^{18}O$ 'zone' of magma, the uppermost sample of nordmarkite analysed has a slightly lower magma $\delta^{18}O$ value than the sample at -4000 m, after which the pulaskites gradually increase in magma $\delta^{18}O$ value with increasing stratigraphic height (Fig. 5). The uppermost foyaite sample that was analysed provides a magma $\delta^{18}O$ value of 5.6 ‰ for both alkali feldspar and pyroxene. The uppermost phonolite magma, therefore, had $\delta^{18}O$ values that are similar to that expected from a mantle-derived magma (5.7 ‰).

The δD value of mantle-derived magmas ought to be about -80 ‰ (Kyser 1986). The δD values of the amphiboles from the Kangerlussuaq Intrusion range from -157 to -86 ‰ (Fig. 4b). The amphiboles analysed in this study are magmatic, with no petrographic evidence of alteration, and the oxygen isotope data are consistent with minimal exchange between the rocks and external fluids. Thus, the amphibole δD values can be used to determine the δD
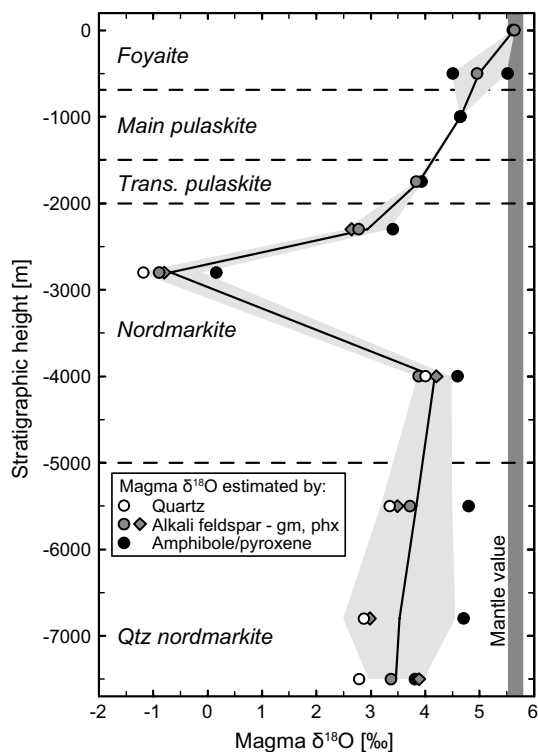
Fig. 5 Magma $\delta^{18}O$ values estimated from various mineral–magma fractionations (see text) against stratigraphic height in the Kangerlussuaq Intrusion. The stratigraphic variation in magma $\delta^{18}O$ is outlined by the black line (with *shaded band* indicating 1σ error) and controlled by either (1) addition of ^{18}O-depleted water to the residual magma by dehydration of basaltic xenoliths or (2) recharge with uncontaminated magma from an underlying chamber

values of the magma. The H-isotope fractionation between amphibole and water depends on the composition of the amphibole and, for the compositional range analysed in the study, should vary from -29 to -52 ‰ (Graham et al. 1984), with the more negative values corresponding to the most Fe-rich amphibole. There is a broad correspondence between changes in amphibole–water content, Mg# and δD value (Fig. 4b, c). However, the difference in $\Delta_{amphibole-water}$ between the most Fe-rich and Fe-poor amphibole (Riishuus et al. 2006) calculated using the equation of Suzuoki and Epstein (1976) is only 23 ‰. This is much less than the measured variation in δD (-157 to -86 ‰). The use of these fractionation factors suggests magma δD values from -105 ‰ in the lower parts of the intrusion and -57 ‰ in the transitional pulaskite.

Previous studies of similar Fe-rich amphiboles in alkaline rocks (e.g. Marks et al. 2004) have reported extremely low δD values (as low as -232 ‰), in apparently magmatic amphibole. Low magma δD values can result from various processes: (1) exchange, assimilation or partial melting of hydrothermally altered country rock, where the alteration

fluid had very low δD values (Taylor 1977), (2) extreme magma degassing (Nabelek et al. 1983; Taylor et al. 1983), (3) exchange between amphibole and deuterium-depleted fluids formed during late-magmatic oxidation of internally produced methane (Marks et al. 2004) or (4) contamination with organic matter or exchange with organic derived fluids (Sheppard 1986). Exchange with methane or organic matter can be excluded because no organic-rich sedimentary rocks occur in the area. Degassing of water during the evolution of the magma is another process that could potentially explain the low δD values of the Kangerlussuaq amphiboles (e.g. Taylor et al. 1983). Nabelek et al. (1983) found that the δD value of hydrous phases in magmatic rocks decreases as the fraction of water initially in the magma decreases during degassing.

The simplest explanation for the low δD values in the nordmarkite magmas is that the H is derived largely from meteoric water. The $\delta^{18}O$ value assumed from ambient meteoric water by Brandriss et al. (1996) is -15 ‰. If this precipitation lies on the global meteoric water line of Craig (1961), its δD value would have been -110 ‰. This value is extremely close to the estimate for the magma δD value of -105 ‰ made for the nordmarkites. This is, therefore, entirely consistent with the model of Pankhurst et al. (1976) wherein large quantities of water of meteoric origin are 'added' to the magma during its evolution.

Origin of low $\delta^{18}O$ magma at Kangerlussuaq

Low-$\delta^{18}O$ magmas (<5.7 ‰) are thought to form by one of two different mechanisms (e.g. Boroughs et al. 2012): (i) partial melting or assimilation of hydrothermally altered material from an earlier stage of volcanism (e.g. Yellowstone; Hildreth et al. 1984; Taylor and Sheppard 1986; Bindeman and Valley 2001; Bindeman et al. 2008) or (ii) partial melting or assimilation of crust that attained low $\delta^{18}O$ values before the onset of magmatism (e.g. the Snake River, USA, Boroughs et al. 2005; Mesozoic granites of E China, Zheng et al. 1998; Rumble et al. 2002; Wei et al. 2008). Mechanism (i) is thought to be related to areas of rifting or large caldera systems (Taylor and Sheppard 1986), and it also appears to be 'visible' only in regions where the ambient meteoric water has highly negative $\delta^{18}O$ values (i.e. high latitudes or high elevation). Mechanism (ii) could, in theory, occur in any magmatic system, but it is limited in practice by the scarcity of low-$\delta^{18}O$ rocks that happen to be in the right P–T–time interval to be partially melted or assimilated.

In the case of the Kangerlussuaq Intrusion, mechanism (ii) is unlikely given that the basement gneisses do not have low $\delta^{18}O$ values. Direct partial melting of the hydrothermally altered tholeiitic basaltic roof material is unlikely to generate a large volume of relatively dry

alkaline trachyte magma. In any case, the basalts are at too high a structural level to have been involved in extensive in situ melting. Brandriss et al. (1996) observed that metabasaltic xenoliths incorporated into the basaltic magma chamber of the Kap Edvard Holm Complex have rounded, crenulated margins, pockets of pegmatitic melt segregations and were depleted in incompatible elements, and argued that the xenoliths underwent dehydration and partial melting. These xenoliths, belonging to the Palaeogene Lower Basalts, are hornfelsed and have $\delta^{18}O$ values as low as -5.5 ‰ (Brandriss et al. 1996). The large variation in $\delta^{18}O$ values and the constant difference between plagioclase and pyroxene $\delta^{18}O$ values for the Kap Edvard Holm xenoliths (Fig. 3d) are consistent with the idea that the xenoliths represent basalt that had interacted with various degrees with low-$\delta^{18}O$ meteoric-hydrothermal fluids before incorporation, and recrystallised in O-isotope equilibrium during heating by the magma (Brandriss et al. 1996).

Like the basaltic xenoliths from the Kap Edvard Holm Complex, those of the Kangerlussuaq Intrusion also once belonged to the Lower Basalts (Riishuus et al. 2008) and have low $\delta^{18}O$ values (-3.2 to 4.6 ‰, Table 1). The low $\delta^{18}O$ values of the Kangerlussuaq Intrusion can be most simply explained by a similar mechanism where the incorporated basaltic material underwent dehydration during assimilation. The basaltic xenoliths from the Kangerlussuaq Intrusion have rounded rims and reaction zones, and the presence of small diffuse mafic bodies in the syenite matrix indicates some digestion of the xenoliths by the trachyte magma. However, sharp contacts between syenite veins and xenolith interiors illustrate that the xenoliths were never hot enough for significant ductile deformation and disintegration that would have led to their complete assimilation. Furthermore, the Kangerlussuaq xenoliths do not show any depletion in LREE elements relative to the Lower Basalts, unlike those from Kap Edvard Holm Complex, and melt segregations are absent (Riishuus et al. 2008). Basalt xenoliths would be less likely to undergo partial melting in a trachytic magma (850–900 °C, depending on water pressure) than in a basaltic magma (~1200 °C) like that of the Kap Edvard Holm Complex. Although the solidus temperature of hydrous basalt is 850–920 °C at 1–3 kb (e.g. Beard and Lofgren 1991), we argue that the basaltic xenoliths that foundered into the Kangerlussuaq magma underwent dehydration without significant partial melting or mechanical assimilation. A potential mechanism to explain the low $\delta^{18}O$ values of the Kangerlussuaq Intrusion magmas is, therefore, the uptake of water derived by the dehydration of xenoliths of hydrated basalt by magma with an initially normal $\delta^{18}O$ value ($\delta^{18}O = 5–7$ ‰).

It is possible to use the simple mass balance equations of Taylor (1977) to model the amount of water required

to interact with the magma to produce the observed shift in $\delta^{18}O$ value. The average $\delta^{18}O$ value of the nordmarkites is ~3.3 ‰ (excluding the sample at -2800 m), and the expected $\delta^{18}O$ value of a fractionated mantle-derived magma can be assumed to be 6.5 ‰, if contaminated by 20 % gneiss (average $\delta^{18}O = 7.8$ ‰), as indicated by the radiogenic isotope data (Riishuus et al. 2008). The Palaeogene meteoric water interacting with the Kap Edvard Holm Complex at ~50 Ma is assumed to have a $\delta^{18}O$ value of ~-15 ‰ (Brandriss et al. 1995). If it is assumed that the system is open and that water continuously percolates upwards through the magma, the single-pass equation of Taylor (1977) is more appropriate than the equation for a closed system. The O-isotope water–magma fractionation factor at 900 °C can be estimated by combining the values of $\Delta_{CO2-melt}$ (5.0 ‰) of Palin et al. (1996), $\Delta_{CO2-calcite}$ (4.4 ‰) of Chacko et al. (1991) and $\Delta_{calcite-water}$ (0.1 ‰) of Clayton et al. (1975), which gives a $\Delta_{water-melt}$ of 0.7 ‰. The water/rock ratio (w/r) calculated in this manner is 0.16 (in atom units) assuming an open system, and this converts to 9 wt% water. It should be emphasised that these represent the integrated amount of water that has to pass through the magma, not the amount of magma that was present in the magma at any one time. This is an extremely large amount of water, as was recognised by Pankhurst et al. (1976) using similar calculations. Table 3 gives the calculated amount of water assuming two different initial magma $\delta^{18}O$ values (6.5 and 5.7 ‰) and water $\delta^{18}O$ values of -15, -20 and -25 ‰. The amount of water required to produce the lowest magma $\delta^{18}O$ value (-1.18 ‰) is also calculated. The calculated water/rock ratio would be lower for more negative $\delta^{18}O$ values of the water and -20 and -25 ‰ give amounts of water of 7 and 6 %, respectively. The same calculations for the lowest magma $\delta^{18}O$ value (quartz 0.7 ‰, magma -1.2 ‰) give amounts of water of 24, 19 and 15 wt%, respectively.

Devolatilisation of stoped blocks and the lowering $\delta^{18}O$ by water fluxing is an attractive mechanism on the grounds of mass balance, water having almost twice as much oxygen by weight than magma, and because it does not rely on diffusion of the water into the magma over large distances, an unrealistically slow process (Taylor and Sheppard 1986). Another advantage of appealing to the addition of water by stoping as opposed to the influx of surface water is that the latter would have descended through, and exchanged with, fractures in heated country rock that would have raised its $\delta^{18}O$ value. Such a process was considered by Bindeman et al. (2008) as a possible cause of low $\delta^{18}O$ values in the Sandwich Horizon of the Skaergaard Intrusion, but was rejected because (a) devolatisation promotes magma crystallisation, and (b) so few xenoliths are observed.

The nature of the altered basalt now represented by the stoped blocks is important to the process. At low

Table 3 Mass balance models for basalt dehydration in the Kangerlussuaq Intrusion

$\delta_{magma,i}$	$\delta_{water,i}$	$\delta_{magma,f}$	Water/rock		wt%
			Closed	Open	Water
6.5	−15	3.3	0.17	0.16	9
6.5	−20	3.3	0.14	0.13	7
6.5	−25	3.3	0.11	0.11	6
6.5	−15	−1.2	0.53	0.42	24
6.5	−20	−1.2	0.39	0.33	19
6.5	−25	−1.2	0.31	0.27	15
5.7	−15	3.3	0.13	0.12	7
5.7	−20	3.3	0.10	0.10	6
5.7	−25	3.3	0.09	0.08	5
5.7	−15	−1.2	0.47	0.39	22
5.7	−20	−1.2	0.35	0.30	17
5.7	−25	−1.2	0.28	0.25	14

$\delta_{magma,i}$ and $\delta_{magma,f}$, initial and final magma $\delta^{18}O$ values; $\delta_{water,i}$, initial $\delta^{18}O$ value of water introduced into magma chamber; water/rock closed and open, water/magma ratio assuming closed and open systems, in atom units; wt% water, amount required in weight%. The $\Delta_{water-magma}$ used was 0.7 ‰ (see text)

temperatures of alteration, the fractionation between minerals and water is large, and the alteration process is much less effective at lowering the $\delta^{18}O$ value of the rock. However, water can be stored in pore spaces and fractures, and the overall water content is potentially high. High temperatures of alteration (>400 °C), by contrast, produce lower $\delta^{18}O$ rocks, because of the smaller fractionation between minerals and water, but the water content will be much lower because of the inherently lower OH content of upper greenschist to amphibolite minerals and the elimination of pore space. Thus, dehydration <u>and</u> assimilation of the altered basalt are required to lower magma $\delta^{18}O$ values. Given the lack of physical evidence for assimilation of the xenoliths, dehydration of hydrated basalt altered at low temperature seems more likely to have occurred.

The amount of water is the sum of water contained in the minerals plus the water that might exist in pore spaces. The porosity of young volcanic rocks is highly variable and can easily be up to 25–35 vol% (Taylor 1986). Manning and Bird (1991) found primary porosities of the Lower Basalts around the Skaergaard intrusion (Fig. 1a) ranging from 0.6 to 10.5 % in massive units and 1.8–22 % in more blocky and fragmented units.

In order to estimate the amount of basalt involved in this process, the water content of the basalt must be known, along with the $\delta^{18}O$ value of the water that is released. Whereas it is possible that very high w/r could occur in the magma immediately surrounding a dehydrating xenolith, it is less easy to understand how the integrated content of

a large magma chamber could be as high as 9 wt%. The water liberated from hydrothermally altered, water-saturated volcanic rocks could have a $\delta^{18}O$ value as low as that of ambient meteoric water (−15 ‰) before dehydration starts. As pointed out by Taylor (1986), rapid dehydration at high temperature would not involve O-isotope equilibration between the liberated water and the restite.

The volume of magma present during formation of the quartz nordmarkites was ~2000 km³ (Riishuus et al. 2008). If the average integrated amount of water required to lower the $\delta^{18}O$ values of the magma was 9 % of the mass of the magma, and the proportion of water present in the foundered basalt was ~10 wt%, the mass of basalt required to be dehydrated is nearly as large as that of the magma. This is almost equivalent to the volume of basalt present above the Kangerlussuaq Intrusion (800 km² × 3–4 km thick; Wager 1947, 1965; Brooks 1979) at the time of its intrusion.

At first glance, such large volumes of water appear unrealistic. Potential explanations that could account for this are as follows:

1. A larger water content in the basalt, which would lower the amount of basalt required to be dehydrated.
2. A much more negative $\delta^{18}O$ value of the water, and a large difference in $\delta^{18}O$ value between the magma and the water. The calculations in Table 3 show that the amount of water would be as low as 5–6 wt%, if the water and magma had $\delta^{18}O$ values of −25 and 5.7–6.5 ‰, respectively.

The porosity of the basaltic rocks that formed the roof of the chamber at the time of intrusion is unknown. There is, however, evidence that this might have been high. Ukstins Peate et al. (2003) reported that 35–40 % of the lower Palaeogene volcanic rocks ('Lower Basalts') of East Greenland consist of primary pyroclastic deposits of basaltic composition, including hyaloclastites. Palagonite can contain up to 25 wt% water (Bonatti 1965), and the presence of relatively unconsolidated sediment would enhance the porosity of the volcanic material. More negative $\delta^{18}O$ values of meteoric water are possible if the period of intense magmatism associated with the initiation produced important regional uplift, the lower $\delta^{18}O$ values being the result of higher altitude. Geomorphological observations (e.g. Brooks 1979) and apatite fission track dating (Gleadow and Brooks 1979; Japsen et al. 2014) suggest massive updoming (>300 km wide, up to ~6 km a.s.l.) in the Kangerlussuaq area beginning at ~51 Ma. Nevle et al. (1994) attributed the low δD values of the hydrothermal water associated with the Kap Edvard Holm Complex to recharge of depleted meteoric waters into deep aquifers above the complex on the flank of the dome. Ambach et al. (1968) report an altitude effect of −0.6 ‰/100 m for Greenland.

Although we cannot use present-day data to determine the isotope composition of precipitation at 50 Ma, these data illustrate that if the elevation of the volcanic edifice was 2000 m above the present height, the $\delta^{18}O$ value of precipitation could have been as low as −27 ‰.

The only alternative mechanism to assimilation of hydrated volcanic material is that the nordmarkite parental magma contained a substantial component of partially melted hydrothermally altered basalt having a low $\delta^{18}O$ value. Simple mixing calculations indicate that addition of 30 % basalt having a $\delta^{18}O$ value of −3.2 ‰ to a mantle-derived magma having a $\delta^{18}O$ value of 6 ‰ would produce a magma having the average $\delta^{18}O$ value of the nordmarkites (~3.3 ‰). It should be emphasised that there is no physical evidence for such a process, although it is possible that altered basalt foundered into a caldera structure whose presence was obliterated by subsequent magmatic activity. Similar models have been adopted to explain the low-$\delta^{18}O$ magmas at Yellowstone (e.g. Bindeman and Valley 2003).

Differentiation of Kangerlussuaq Intrusion magmas

The close association of silica undersaturated and oversaturated magmas at Kangerlussuaq was explained by Riishuus et al. (2008) as being due to the magma chamber being initially filled by differentiated alkali basalt magma that had assimilated lower crust. Thereafter, the magma chamber was recharged by differentiated but progressively less contaminated phonolitic magmas. These magmas filling the Kangerlussuaq magma chamber were assumed to originate from a deep-seated magma chamber. The influx of progressively less contaminated magmas resulted from the gradual armouring of the walls and conduit(s) by congealed magma, which prevented further contamination. However, this model does not explain how the continuous transfer of these differentiated magmas into the Kangerlussuaq Intrusion magma chamber can result in a gradual change from quartz nordmarkite to foyaite.

Increasing the amount of water dissolved in magmas in the system Ne–Ks–Q–H_2O has the effect of depressing all liquidus surfaces, including the Ab–Or join (Fig. 6) that constitutes a thermal divide (e.g. Morse 1969; Tuttle and Bowen 1958). Increasing the water content of the magma permits a superheated liquid to cross the thermal divide during mixing with a silica undersaturated melt, as suggested by Riishuus et al. (2008). Without addition of water, mixing of a silica oversaturated residual liquid with silica undersaturated recharging magma would result in sudden crystallisation, unless the recharging magma was hot enough to for the bulk magma to remain superheated.

Kempe and Deer (1970) estimated liquidus temperatures of approximately 760–80 °C for the foyaites and ~880 °C
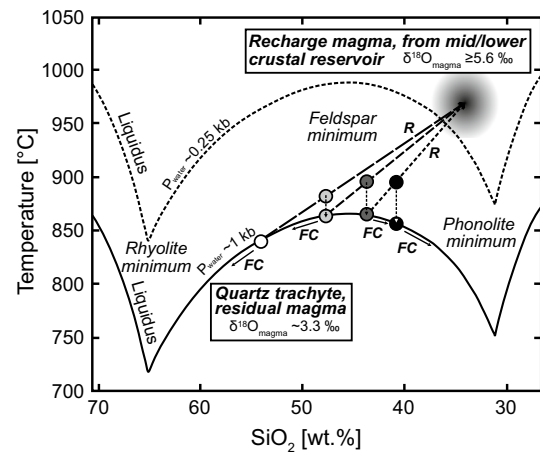
Fig. 6 Schematic illustration of profiles along minima in petrogeny's residua system. The profile for $pH_2O = 1$ kbar is from Morse (1969) (after Tuttle and Bowen 1958; Hamilton and MacKenzie 1965). The shape of the profile at $pH_2O = 0.25$ kbar is for simplicity identical to that at 1 kbar, but shifted so that the feldspar minimum lies at the correct temperature (see Fig. 26 in Tuttle and Bowen (1958)). The arrows and symbols illustrate a possible T–X path taken by an initially silica oversaturated quartz trachytic magma at pH_2O ~1 kbar (water saturated) in the Kangerlussuaq magma chamber following intermittent episodes of magmatic recharge (*R*) with a superheated, silica undersaturated magma (here phonolitic) and fractional crystallisation (FC), gradually forcing a compositional change across the feldspar minimum towards lower silica content. See text for detailed account

for the main pulaskite using the nepheline geothermometer of Hamilton (1961). Single-feldspar thermometry using the bulk perthite compositions from Kempe and Deer (1970) and the temperature-dependent feldspar solvus of Fuhrman and Lindsley (1988) at 1 kbar yields temperatures of 800–850 °C for nordmarkites and pulaskites and 750–800 °C for foyaites. These temperature estimates suggest water-saturated conditions throughout the formation of the exposed cumulate sequence of ~1 kbar (Fig. 6), and that the pH_2O of the KI magma chamber was equal to the lithostatic pressure.

We argue that lowering of the liquidus in response to the uptake of water derived from dehydrating basalt xenoliths allowed mixing between the residual silica oversaturated magma in the KI chamber with recharging silica undersaturated magma at temperatures above the feldspar thermal divide (Fig. 6). This would result in intermittent superheated conditions in the KI magma chamber followed by a return to liquidus conditions and continued crystallisation. The gradual mineralogical, elemental and isotopic changes from quartz nordmarkite through foyaite (Riishuus et al. 2008; this study) imply that magma recharge was more frequent than we have schematically illustrated in Fig. 6. Recharge must have been frequent enough to prevent fractionation towards the rhyolite minimum, thereby

gradually forcing the residual magma closer to, and eventually across, the feldspar minimum. Basaltic xenoliths disappear from the stratigraphy at the level of the pulaskites, and from this stage of crystallisation onwards, no external water was added to the magma chamber, and the magma $\delta^{18}O$ becomes 'normal'. The residual magma would at this stage be able to fractionate towards the phonolite minimum (Fig. 6).

Conclusions

1. The $\delta^{18}O$ values of coexisting alkali feldspar, quartz and amphibole/pyroxene in the Kangerlussuaq Intrusion are consistent with O-isotope equilibrium at magmatic temperatures.

2. The upper silica undersaturated rocks crystallised from magmas with $\delta^{18}O$ values close to that expected for a mantle-derived magma. The silica oversaturated rocks crystallised from magma with an average $\delta^{18}O$ value of ~3.3 ‰ and represent a large volume (2000 km^3) of low-$\delta^{18}O$ magma. One sample crystallised from magma with a $\delta^{18}O$ value as low as −1.2 ‰, but this is of unknown extent, and could represent only a small volume of magma.

3. The low-$\delta^{18}O$ nordmarkitic magma had a δD value of −105 ‰, which is lower than that expected for a mantle-derived magma (−60 to −80 ‰) but similar to ambient meteoric water.

4. Incorporation and rapid dehydration of water-rich altered basalt roof rocks that foundered into the magma by stoping is the most viable mechanism that could explain the low $\delta^{18}O$ values of the nordmarkite magmas. Mass balance calculations indicate that the integrated amount of water that would have to pass through the magma by far exceeds the amount of water present in the magma at any one time. Water introduced in this way could, however, account for the low δD value of the nordmarkitic magmas and account for the magma with the lowest $\delta^{18}O$ value, if the magma exchanged with ~30 wt% of water, and the volume of this low-$\delta^{18}O$ 'horizon' is relatively small.

5. The magmas that filled the KI magma chamber originated as alkali basalt that became contaminated at deep crustal levels resulting in initially silica oversaturated magma. This magma was emplaced in the upper crust and stoped its way into a roof of hydrothermally altered basalts, which foundered into the magma chamber. Quartz nordmarkite cumulates crystallised, and the water introduced by dehydrating basaltic xenoliths raised pH_2O of the magma to ~1 kbar. Depression of the liquidus as a result of increasing water content, accompanied by the influx of progressively less con-

taminated silica undersaturated magmas, facilitated the gradual change from nordmarkite cumulates to pulaskite and foyaites at a temperature above the feldspar thermal divide. It therefore appears that the KI magma chamber was a dynamic open system, with concurrent dehydration of basaltic xenoliths, magmatic recharge and escape of water through the roof.

References

Ambach W, Dansgaard W, Eisner H, Moller J (1968) The altitude effect on the isotopic composition of precipitation and glacier ice in the Alps. Tellus 20:594–600

Beard JS, Lofgren GE (1991) Dehydration melting and water-saturated melting of basaltic and andesitic greenstones and amphibolites at 1, 3, and 6.9 kb. J Petrol 32:365–401

Bindeman I (2008) Oxygen isotopes in mantle and crustal magmas as revealed by single crystal analysis. Rev Mineral Geochem 69(1):445–478

Bindeman IN, Valley JW (2001) Low-$\delta^{18}O$ rhyolites from Yellowstone: magmatic evolution based on analyses of zircon and individual phenocrysts. J Petrol 42:1491–1517

Bindeman IN, Valley JW (2003) Rapid generation of both high- and low-$\delta^{18}O$, large volume silicic magmas at Timber Mountain/Oasis Valley caldera complex, Nevada. Geol Soc Am Bull 115(5):581–595

Bindeman IN, Fu B, Kita NT, Valley JW (2008) Origin and evolution of silicic magmatism at Yellowstone based on ion microprobe analysis of isotopically zoned zircons. J Petrol 49:163–193

Bonatti E (1965) Palagonite, hyaloclastites and alteration of volcanic glass in the ocean. Bull Volc 28:257–269

Boroughs S, Wolff J, Bonnichsen B, Godchaux M, Larson P (2005) Large-volume, low-delta O-18 rhyolites of the central Snake River Plain, Idaho, USA. Geology 33:821–824

Boroughs S, Wolff JA, Ellis BS, Bonnichsen B, Larson PB (2012) Evaluation of models for the origin of Miocene low-delta O-18 rhyolites of the Yellowstone/Columbia River Large Igneous Province. Earth Planet Sci Lett 313:45–55

Brandriss ME, Nevle RJ, Bird DK, O'Neil JR (1995) Imprint of meteoric water on the stable isotope compositions of igneous and secondary minerals, Kap Edvard Holm Complex, East Greenland. Contrib Mineral Petrol 121:74–86

Brandriss ME, Bird DK, O'Neil JR, Cullers RL (1996) Dehydration, partial melting, and assimilation of metabasaltic xenoliths in gabbros of the Kap Edvard Holm complex, East Greenland. Am J Sci 296:333–393

Brooks CK (1973) Rifting and doming in southern East Greenland. Nature 244:23–25

Brooks CK (1979) Geomorphological observations at Kangerdlugssuaq, East Greenland. Medd Grønland Geosci 1:1–21

Brooks CK, Gill RCO (1982) Compositional variation in the pyroxenes and amphiboles of the Kangerdlugssuaq Intrusion, East Greenland: further evidence for the crustal contamination of syenite magma. Mineral Mag 45:1–9

Brooks CK, Nielsen TFD (1982a) The E Greenland continental margin: a transition between oceanic and continental magmatism. J Geol Soc Lond 139:265–275

Brooks CK, Nielsen TFD (1982b) The Phanerozoic development of the Kangerdlugssuaq area, East Greenland. Medd Grønland Geosci 9:1–30

Chacko T, Mayeda TK, Clayton RN, Goldsmith JR (1991) Oxygen and carbon isotope fractionations between CO_2 and calcite. Geochim Cosmochim Acta 55:2867–2882

Chiba H, Chacko T, Clayton RN, Goldsmith JR (1989) Oxygen isotope fractionations involving diopside, forsterite, magnetite, and calcite: application to geothermometry. Geochim Cosmochim Acta 53:2985–2995

Clayton RN, Goldsmith JR, Karel KJ, Mayeda TK, Newton RC (1975) Limits on the effect of pressure on isotopic fractionation. Geochim Cosmochim Acta 39:1197–1201

Clayton RN, Goldsmith JR, Mayeda TK (1989) Oxygen isotope fractionation in quartz, albite, anorthite and calcite. Geochim Cosmochim Acta 53:725–733

Coplen TB (1988) Normalization of oxygen and hydrogen isotope data. Chem Geol 72:293–297

Craig H (1961) Isotopic variations in meteoric waters. Science 133:1702–1703

Deer WA, Kempe DRC (1976) Geological investigations in East Greenland, Part XI, The minor peripheral intrusions, Kangerdlugssuaq, East Greenland. Medd Grønland 197(4):1–25

Eiler JM (2001) Oxygen isotope variations of basaltic lavas and upper mantle rocks. Rev Mineral 43:319–364

Fagereng A, Harris C, La Grange M, Stevens G (2008) Stable isotope study of the Archaean rocks of the Vredefort impact structure, central Kaapvaal craton, South Africa. Contrib Mineral Petrol 155:63–78

Fuhrman ML, Lindsley DH (1988) Ternary-feldspar modeling and thermometry. Am Mineral 73:201–215

Giletti BJ (1986) Diffusion effects on oxygen isotope temperatures of slowly cooled igneous and metamorphic rocks. Earth Planet Sci Lett 77:218–228

Gleadow AJW, Brooks CK (1979) Fission track dating, thermal histories and tectonics of igneous intrusions in East Greenland. Contrib Mineral Petrol 71:45–60

Graham CM, Harmon RS, Sheppard SMF (1984) Experimental hydrogen isotope studies: hydrogen isotope exchange between amphibole and water. Am Mineral 69:128–138

Gregory RT, Criss RE (1986) Isotopic exchange in open and closed systems. In: Valley JW, Taylor HP Jr, O'Neil JR (eds) Stable isotopes in high-temperature geological processes, vol 16. Mineralogical Society of America, Washington, pp 91–127

Hamilton DL (1961) Nephelines as crystallization temperature indicators. J Geol 69:321–329

Hamilton DL, MacKenzie WS (1965) Phase-equilibrium studies in the system $NaAlSiO_4$ (nepheline)–$KAlSiO_4$ (kalsilite)–SiO_2–H_2O. Mineral Mag 34:214–231

Hansen H, Pedersen AK, Duncan RA, Bird DK, Brooks CK, Fawcett JJ, Gittins J, Gorton M, O'Day P (2002) Volcanic stratigraphy of the southern Prinsen af Wales Bjerge region, East Greenland. In: Jolley DW, Bell BR (eds) The North Atlantic Igneous Province: stratigraphy, tectonic, volcanic and magmatic processes, vol 197. Geological Society, London, Special Publications, pp 183–218

Harris C (1995) Oxygen isotope geochemistry of the Mesozoic anorogenic complexes of Damaraland, northwest Namibia: evidence for crustal contamination and its effect on silica saturation. Contrib Mineral Petrol 122:308–321

Harris C, Grantham GH (1993) Geology and petrogenesis of the Straumsvola nepheline syenite complex, Dronning Maud Land, Antarctica. Geol Mag 130:513–532

Hildreth W, Christiansen RL, O'Neil JR (1984) Catastrophic isotopic modification of rhyolitic magma at times of caldera subsidence, Yellowstone Plateau volcanic field. J Geophys Res 89:8339–8369

Japsen P, Green PF, Bonow JM, Nielsen TFD, Chalmers JA (2014) From volcanic plains to glaciated peaks: Burial, uplift and exhumation history of southern East Greenland after opening of the NE Atlantic. Global Planet Change 116:91–114

Jenkins GRT, Fallick AE, Farrow CM, Bowes GM (1991) COOL: a FORTRAN 77 computer program for modelling stable isotopes in cooling closed systems. Comput Geosci 17:391–412

Kempe DRC, Deer WA (1970) Geological investigations in East Greenland, part IX, The mineralogy of the Kangerdlugssuaq alkaline intrusion, East Greenland. Medd Grønland 190(3):1–97

Kempe DRC, Deer WA (1976) The petrogenesis of the Kangerdlugssuaq alkaline intrusion, East Greenland. Lithos 9:111–123

Kempe DRC, Deer WA, Wager LR (1970) Geological investigations in East Greenland, part VIII, The petrology of the Kangerdlugssuaq alkaline intrusion, East Greenland. Medd Grønland 190(2):1–52

Kyser TK (1986) Stable isotope variations in the mantle. In: Valley JW, Taylor HP Jr, O'Neil JR (eds) Stable isotopes in high-temperature geological processes, vol 16. Mineralogical Society of America, Washington, pp 141–164

Lackey JS, Valley JW, Chen JH, Stockli DF (2008) Dynamic magma systems, crustal recycling, and alteration in the central Sierra Nevada batholith: the oxygen isotope record. J Petrol 49:1397–1426

Larsen LM, Watt WS, Watt M (1989) Geology and petrology of the lower Tertiary plateau basalts of the Scoresby Sund region, East Greenland. Geol Surv Greenl Bull 157:1–164

Manning CE, Bird DK (1991) Porosity evolution and fluid flow in the basalts of the Skaergaard magma-hydrothermal system, East Greenland. Am J Sci 291:201–257

Marks M, Vennemann T, Siebel W, Markl G (2004) Nd-, O- and H-isotopic evidence for complex, closed-system fluid evolution of the peralkaline Ilímaussaq intrusion, South Greenland. Geochim Cosmochim Acta 68:3379–3395

Morse SA (1969) Syenites. Carnegie Institution of Washington Annual Report Geophysical Laboratory vol 67, pp 112–120

Nabelek PI, O'Neil JR, Papike JJ (1983) Vapor phase exsolution as a controlling factor in hydrogen isotope variation in granitic rocks: the Notch Peak granitic stock, Utah. Earth Planet Sci Lett 66:137–150

Nevle RJ, Brandriss ME, Bird DK, McWilliams MO, O'Neil JR (1994) Tertiary plutons monitor climate change in East Greenland. Geology 22:775–778

Nielsen TFD (1987) Tertiary alkaline magmatism in East Greenland: a review. In: Fitton JG, Upton BGJ (eds) Alkaline Igneous rocks, vol 30. Blackwell, Oxford, pp 489–515

Palin JM, Epstein S, Stolper EM (1996) Oxygen isotope partitioning between rhyolitic glass/melt and CO_2: an experimental study at 550–950°C and 1 bar. Geochim Cosmochim Acta 60:1963–1973

Pankhurst RJ, Beckinsale RD, Brooks CK (1976) Strontium and oxygen isotope evidence relating to the petrogenesis of the Kangerdlugssuaq alkaline intrusion, East Greenland. Contrib Mineral Petrol 54:17–42

Peate DW, Baker JA, Blichert-Toft J, Hilton DR, Storey M, Kent AJR, Brooks CK, Hansen H, Pedersen AK, Duncan RA (2003) The Prinsen af Wales Bjerge Formation lavas, East Greenland: the

transition from tholeiitic to alkalic magmatism during Palaeogene continental break-up. J Petrol 44:279–304

Pedersen AK, Watt M, Watt WS, Larsen LM (1997) Structure and stratigraphy of the early Tertiary basalts of the Blosseville Kyst, East Greenland. J Geol Soc London 154:565–570

Riishuus MS, Peate DW, Tegner C, Wilson JR, Brooks CK, Waight TE (2005) Petrogenesis of syenites at a rifted continental margin: origin, contamination and interaction of alkaline mafic and felsic magmas in the Astrophyllite Bay Complex, East Greenland. Contrib Mineral Petrol 149:350–371

Riishuus MS, Peate DW, Tegner C, Wilson JR, Brooks CK, Harris C (2006) Temporal evolution of a long-lived syenitic centre: the Kangerlussuaq Alkaline Complex, East Greenland. Lithos 92:276–299

Riishuus MS, Peate DW, Tegner C, Wilson JR, Brooks CK (2008) Petrogenesis of cogenetic silica-oversaturated and undersaturated syenites by periodic recharge in a crustally contaminated magma chamber: the Kangerlussuaq Intrusion, East Greenland. J Petrol 49:493–522

Rose NM (1989) Geochemistry of hydrothermal metasomatism in basaltic systems. PhD. Stanford University, 188 pp

Rumble D, Giorgis D, Ireland T, Zhang ZM, Xu HF, Yui TF, Yang JS, Xu ZQ, Liou JG (2002) Low delta O-18 zircons, U-Pb dating, and the age of the Qinglongshan oxygen and hydrogen isotope anomaly near Donghai in Jiangsu Province, China. Geochim Cosmochim Acta 66:2299–2306

Saunders AD, Fitton JG, Kerr AC, Norry MJ, Kent RW (1997) The North Atlantic Igneous Province. In: Mahoney JJ, Coffin MF (eds) Large Igneous Provinces: continental, oceanic, and planetary flood volcanism, vol 100. American Geophysical Union, Washington, pp 45–93

Schairer JF (1950) The alkali-feldspar join in the system $NaAlSiO_4$–$KAlSiO_4$–SiO_2. J Geol 58:512–517

Sheppard SMF (1986) Igneous rocks: III. Isotopic case studies of magmatism in Africa, Eurasia and oceanic islands. In: Valley JW, Taylor HP Jr, O'Neil JR (eds) Stable isotopes in high-temperature geological processes, vol 16. Mineralogical Society of America, Washington, pp 319–371

Sheppard SMF, Brown PE, Chambers AD (1977) Lilloise intrusion, East Greenland—hydrogen isotope evidence for efflux of magmatic water into contact metamorphic aureole. Contrib Mineral Petrol 63:129–147

Storey M, Duncan RA, Tegner C (2007) Timing and duration of volcanism in the North Atlantic Igneous Province: implications for geodynamics and links to the Iceland hotspot. Chem Geol 241:264–281

Suzuoki T, Epstein S (1976) Hydrogen isotope fractionation between OH-bearing minerals and water. Geochim Cosmochim Acta 40:1229–1240

Taylor HP Jr (1968) The oxygen isotope geochemistry of igneous rocks. Contrib Mineral Petrol 19:1–71

Taylor HP Jr (1977) Water/rock interactions and the origin of H_2O in granitic batholiths. J Geol Soc London 133:509–558

Taylor HP Jr (1986) Igneous rocks: II. Isotopic case studies of Circumpacific magmatism. In: Valley JW, Taylor HP Jr, O'Neil JR (eds) Stable isotopes in high-temperature geological processes, vol 16. Mineralogical Society of America, Washington, pp 273–317

Taylor HP Jr, Forester RW (1979) An oxygen and hydrogen isotope study of the Skaergaard intrusion and its country rocks: a description of a 55 m.y. old fossil hydrothermal system. J Petrol 20:355–419

Taylor HP Jr, Sheppard SMF (1986) Igneous rocks: I. Processes of isotopic fractionation and isotope systematics. In: Valley JW, Taylor HP Jr, O'Neil JR (eds) Stable isotopes in high-temperature geological processes, vol 16. Mineralogical Society of America, Washington, pp 227–271

Taylor BE, Eichelberger JC, Westrich HR (1983) Hydrogen isotope evidence of rhyolitic magma degassing during shallow intrusion and eruption. Nature 306:541–545

Tegner C, Brooks CK, Duncan RA, Heister LE, Bernstein S (2008) 40Ar-39Ar ages of intrusions in East Greenland: rift-to-drift transition over the Iceland hotspot. Lithos 101(3–4):480–500

Tuttle OF, Bowen NL (1958) Origin of granite in the light of experimental studies in the system $NaAlSiO_4$–$KAlSiO_4$–SiO_2–H_2O. GSA Mem 74:1–153

Ukstins Peate IU, Larsen M, Lesher CE (2003) The transition from sedimentation to flood volcanism in the Kangerlussuaq Basin, East Greenland: basaltic pyroclastic volcanism during initial Palaeogene continental break-up. J Geol Soc London 160:759–772

Vennemann TW, O'Neil JR (1993) A simple and inexpensive method of hydrogen isotope and water analyses of minerals and rocks based on zinc reagent. Chem Geol 103:227–234

Vennemann TW, Smith HS (1990) The rate and temperature of reaction of ClF_3 with silicate minerals, and their relevance to oxygen isotope analysis. Chem Geol 86:83–88

Vennemann TW, Smith HS (1992) Stable isotope profile across the orthoamphibole isograd in the Southern Marginal Zone of the Limpopo Belt, South Africa. Precambr Res 55:365–397

Verhoef J, Roest WR, Macnab R, Arkani-Hamed J (1996) Magnetic anomalies of the Arctic and North Atlantic oceans and adjacent land areas. Geological Survey of Canada, Open File 3125

Wager LR (1947) Geological investigations in East Greenland, Part IV: the stratigraphy and tectonics of Knud Rasmussens Land and the Kangerdlugssuaq region. Medd Grønland 134:1–64

Wager LR (1965) The form and internal structure of the alkaline Kangerdlugssuaq intrusion, East Greenland. Mineral Mag 34:487–497

Wei CS, Zhao ZF, Spicuzza MJ (2008) Zircon oxygen isotopic constraint on the sources of late Mesozoic A-type granites in eastern China. Chem Geol 250:1–15

Wotzlaw JF, Bindeman IN, Schaltegger U, Brooks CK, Naslund HR (2012) High-resolution insights into episodes of crystallization, hydrothermal alteration and remelting in the Skaergaard intrusive complex. Earth Planet Sci Lett 355–356:199–212

Zhao ZF, Zheng YF (2003) Calculation of oxygen isotope fractionation in magmatic rocks. Chem Geol 193(1–2):59–80

Zheng Y-F (1993a) Calculation of oxygen isotope fractionation in anhydrous silicate minerals. Geochim Cosmochim Acta 57:1079–1091

Zheng Y-F (1993b) Calculation of oxygen isotope fractionation in hydroxyl-bearing silicates. Earth Planet Sci Lett 120:247–263

Zheng YF, Fu B, Li YL, Xiao YL, Li SG (1998) Oxygen and hydrogen isotope geochemistry of ultrahigh-pressure eclogites from the Dabie Mountains and the Sulu terrane. Earth Planet Sci Lett 155(1–2):113–129